

Topology of magnetic field lines: Chaos and bifurcations emerging from two-action systemsTomoshige Miyaguchi,^{1,*} Makoto Hosoda,¹ Katsuyuki Imagawa,¹ and Katsuhiro Nakamura^{1,2}¹*Department of Applied Physics, Graduate School of Engineering, Osaka City University, Osaka 558-8585, Japan*²*Heat Physics Department, Uzbek Academy of Sciences, 28 Kataltal Street, 100135 Tashkent, Uzbekistan*

(Received 19 April 2010; revised manuscript received 30 July 2010; published 6 January 2011)

Nonlinear dynamics of magnetic field lines generated by simple electric current elements are investigated. In general, the magnetic field lines show behavior similar to that of the Hamiltonian systems; in fact, they can be generally transformed into Hamiltonian systems with 1.5 degrees of freedom, obey the Kolmogorov-Arnold-Moser (KAM) theorem, and generate chaotic trajectories. In the case where unperturbed systems are described by two action (slow) and one angle (fast) variables, however, it is found that the periodic orbits of the unperturbed systems vanish for arbitrarily small symmetry-breaking perturbations (a breakdown of the KAM theorem) and drifting or periodic trajectories appear. The mechanism of this phenomenon is investigated analytically by weak nonlinear stability analysis. It is also shown numerically that scattering processes of the perturbed system exhibit typical features of chaotic dynamical systems.

DOI: [10.1103/PhysRevE.83.016205](https://doi.org/10.1103/PhysRevE.83.016205)

PACS number(s): 05.45.–a

I. INTRODUCTION

Although the phase space dimensions of Hamiltonian systems are of even order, there are also conservative dynamical systems with odd dimensions. Among such systems, three-dimensional volume-preserving flows and maps are the most important, because they are associated with many physical phenomena. For example, the ordinary differential equations describing magnetic field lines (MFLs) are volume preserving—namely, the vector fields are divergence-free [1–3]. Since MFLs are common tools for visualization of magnetic fields [4,5], from the viewpoint of applications it is important to understand their dynamics. In addition, MFLs play an essential role in understanding the confinement of tokamak plasma [1,6–8], and studies of chaotic phenomena in Hamiltonian systems were strongly motivated by the practical importance of MFLs in plasma physics. One prominent characteristic of MFLs is that they are conservative systems with no approximation, because MFLs are defined simply by the stream lines of magnetic fields, which are divergence-free. Another famous example of a volume-preserving system is passive scalars (PSs) in incompressible fluid flows [9,10]. The dynamics of PSs are also an important field of research because of their significance in combustion and chemical reactions, and therefore they have been intensively investigated [9–15] since the pioneering work by Arnold who studied the so-called ABC flow [16]. However, the dynamics of PSs are different from those of MFLs in that the equations for PSs are derived by neglecting thermal fluctuations and the influence of PSs on the fluids [9].

Three-dimensional volume-preserving flows and maps can be classified according to the number of action (slow) variables. In the case where an unperturbed system has only one action variable (action-angle-angle case), the general methods and theorems for Hamiltonian systems such as the Melnikov method and Kolmogorov-Arnold-Moser (KAM) theorem can be applied [17], and therefore the perturbed system generally exhibits chaotic behavior similar to that in Hamiltonian

systems. For example, in recent studies [2,3,18], chaotic MFLs created by several current elements were investigated and found to be generated by realistic current configurations. In particular, in Ref. [3], it was demonstrated numerically that electric circuits such as power wires and printed circuit boards can also produce chaotic MFLs, and in Ref. [2], chaotic MFLs generated through a scenario based on the Poincaré-Birkhoff theorem [19] were studied. In the case where the unperturbed system has two action variables (action-action-angle case), however, the behavior of the perturbed system is different from that of generic Hamiltonian systems; for example the KAM theorem does not always hold [20]. This two-action case has already been studied on PSs [9,17,20–22], but, to the authors' knowledge, there has been no investigation on MFLs. The main purpose of the present paper is therefore to examine the nonlinear dynamics of MFLs for the two-action case.

This paper is organized as follows. In Sec. II, we study the topology of MFLs of a system with a single coil and a straight wire. We introduce the ordinary differential equations describing the MFLs of this system, and show numerical results for both one- and two-action systems. Moreover it is shown that the periodic orbits of the unperturbed system vanish for arbitrarily small perturbations for the two-action case. The mechanism of this phenomenon is studied analytically by weak nonlinear stability analysis using a Lyapunov function. The scattering process of the perturbed two-action system is also studied and it is shown that some features typical in chaotic dynamical systems appear in this scattering process. In Sec. III, we show numerical results for a system with two coils and a straight wire; this system has a hyperbolic fixed point and shows more complex behavior than the single coil system. Finally, Sec. IV is devoted to a conclusion.

II. SINGLE COIL SYSTEM

A magnetic field line $\mathbf{r}(\tau) \in \mathcal{R}^3$, parametrized by a pseudo-time-variable τ obeys the ordinary differential equation $\dot{\mathbf{r}} = \mathbf{B}$ [7,8], where \mathbf{B} is the magnetic field. Let us begin with a system with a single coil and a straight wire, as shown in Fig. 1(a).

*tomo@a-phys.eng.osaka-cu.ac.jp

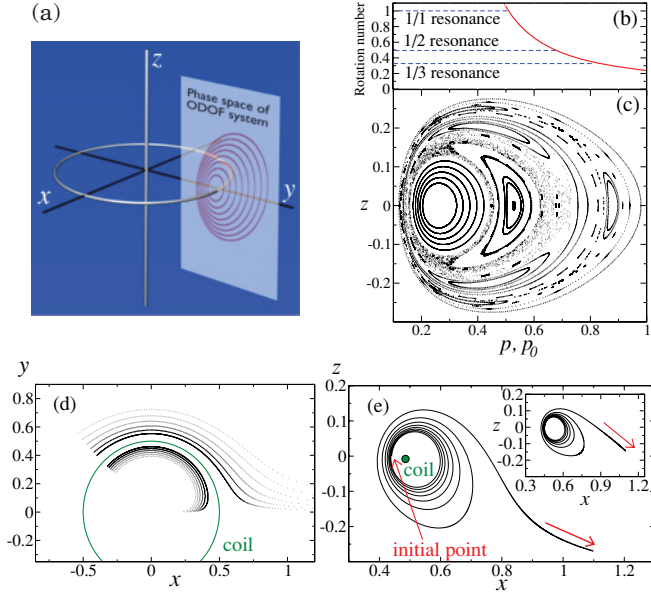


FIG. 1. (Color online) (a) The wire configuration of the single coil system. (b) and (c) The rotation number and the Poincaré section $\phi = \pi/2$ in the one-action case. Parameters are set as $I_C = 0.1, I_L = 1.0$, and $B_x = 0.005$. (d) For the two-action case, the Poincaré section $z = 0$ is shown for six orbits that start at points $(-r_0/\sqrt{2}, r_0/\sqrt{2}, 0)$ ($0.38 \leq r_0 \leq 0.455$). The parameter values are $I_C = 0.1, I_L = 0.0$, and $B_x = 0.001$. (e) A typical orbit in the invariant subspace $\phi = 0$. The parameter values are the same as in (d) except that $B = 0.02$. (Inset) An orbit of the approximated equations (4) and (5).

The magnetic field lines for this system can be described by the following equations:

$$\dot{z} = \frac{1}{r} \frac{\partial(rA_\phi)}{\partial r}, \quad \dot{r} = -\frac{\partial A_\phi}{\partial z}, \quad \dot{\phi} = \tilde{\Omega}_L(r), \quad (1)$$

where (z, r, ϕ) are the cylindrical coordinates. In Eqs. (1), the function $\tilde{\Omega}_L(r)$, which is the contribution from the linear current along the straight wire, is defined as $\tilde{\Omega}_L(r) = \mu_0 I_L / (2\pi r^2)$, where μ_0 and I_L are the permeability and the intensity of the linear current, respectively. The function $A_\phi(z, r, \phi)$ is the ϕ component of the vector potential of the coil, which is expressed using the complete elliptic functions of the first and second kinds, $K(k)$ and $E(k)$, as follows [23,24]:

$$A_\phi(z, r, \phi) = \frac{\mu_0 I_C}{\pi k} \left(\frac{a}{r}\right)^{\frac{1}{2}} \left[\left(1 - \frac{1}{2}k^2\right) K(k) - E(k) \right], \quad (2)$$

where the variable k is defined by $k^2 = 4ar / [(a+r)^2 + z^2]$, and the parameters a and I_C are the radius and the current intensity of the coil, respectively. In all of the following numerical simulations, we set $a = 0.5$ and $\mu_0 = 1.0$. In Eq. (1), let us change the variables as $q = z$ and $p = r^2$, so that

$$\dot{q} = \frac{\partial H}{\partial p}(q, p), \quad \dot{p} = -\frac{\partial H}{\partial q}(q, p), \quad \dot{\phi} = \Omega_L(p), \quad (3)$$

where the Hamiltonian $H(q, p)$ is defined by $H(q, p) := 2rA_\phi$ and the function $\Omega_L(p)$ by $\Omega_L(p) := \tilde{\Omega}_L(r(p))$. In Eq. (3), q and p are the canonical variables of the one-degree-of-freedom

Hamiltonian $H(q, p)$. This transformation into the integrable Hamiltonian system is a consequence of the continuous rotational symmetry [17,25]. Note that in the case where $I_L = 0$, ϕ is a constant, and hence the system has two slow variables, ϕ and the action variable defined for the one-degree-of-freedom Hamiltonian system $H(q, p)$ (a two-action case). In the case where $I_L \neq 0$, however, ϕ is a fast variable, and hence the system has only one slow variable (a one-action case).

In the one-action case, in which $I_L \neq 0$, the effect of perturbations to the system has been studied in the context of plasma physics [6–8], and also in a recent paper [2]. In the present paper, in order to compare with the two-action case described below, the behavior of a one-action system under a perturbation is first briefly explained. We adopt a uniform magnetic field in the x direction, $\mathbf{B} = (B_x, 0, 0)$, as a perturbation—the type of the perturbation is not important as long as it breaks the rotational symmetry. Note also that this perturbation can be considered as being weak only in a region near the coil. A Poincaré surface $\phi = \pi/2$ is shown in Fig. 1(a); in this case, the unperturbed nonresonant orbits form two-dimensional invariant surfaces. In Fig. 1(b), the rotation number $\rho(p_0)$ of the unperturbed orbit starting at the point $(q, p, \phi) = (0, p_0, \pi/2)$ is displayed as a function of p_0 . More precisely, $\rho(p_0)$ is defined by the number of rotations around the coil during one iteration of the Poincaré map. Figure 1(c) is the Poincaré surface under the perturbation; from this figure, it is clear that chains of island tori are formed in a neighborhood of the resonant torus of the unperturbed system, and that chaotic orbits fill the regions between these island tori. Therefore, in this case, the chaos can be considered to be generated through the Poincaré-Birkhoff type scenario.

The behavior of MFLs in the two-action case, in which $I_L = 0$, is different from that in the one-action case. In the two-action case, the variable ϕ is constant for unperturbed flow and hence the periodic orbits in the unperturbed system are one-dimensional closed curves, and none of them form two-dimensional invariant surfaces. Under arbitrarily weak perturbations of the uniform magnetic field, $B_x > 0$, the orbits drift in the x direction, transiently forming spirals, and then escape to infinity as shown in Fig. 1(d), where Poincaré section $z = 0$ is plotted for six trajectories started from $(-r_0/\sqrt{2}, r_0/\sqrt{2}, 0)$ ($0.38 \leq r_0 \leq 0.455$). In the numerical simulations, all the periodic orbits of the unperturbed systems vanished in this manner for arbitrarily small perturbations; this contrasts with the situation for the one-action case described above, in which the KAM theorem ensures the preservation of nonresonant tori under weak perturbations. This instability in two-action systems can be well understood by analyzing the dynamics on the xz plane with $x > 0$, which is an invariant subspace of the perturbed system. On this subspace, the orbits initially located near the coil spiral out from the singular point $(z, x) = (0, a)$ as shown in Fig. 1(e). For $B_x < 0$, however, the orbits spiral into the point. Thus the stability around the point $(z, x) = (0, a)$ bifurcates at $B_x = 0$.

For the purpose of clarifying this bifurcation, we derive approximate equations near the point $(z, x) = (0, a)$. Because the equation for ϕ is given by $\dot{\phi} = -B_x \sin(\phi)$, it is obvious that $\phi = 0$ ($\phi = \pi$) is a stable (unstable) subspace with respect to ϕ . Let us consider the equations for the orbits inside the

subspace $\phi = 0$. Using the infinitesimal quantities \tilde{z} and \tilde{x} defined by $z = \tilde{z}$ and $r = x = a + \tilde{x}$, the orbits near the point, $(z, x) = (0, a)$ are described by the following equations:

$$\dot{\tilde{z}} = -\frac{C\tilde{x}}{\tilde{z}^2 + \tilde{x}^2} - \frac{C}{2a} \ln(\tilde{z}^2 + \tilde{x}^2), \quad (4)$$

$$\dot{\tilde{x}} = \frac{C\tilde{z}}{\tilde{z}^2 + \tilde{x}^2} + B_x, \quad (5)$$

where $C = \mu_0 I_C / 2\pi$ is a constant. The first terms of the right hand sides of Eqs. (4) and (5) are the leading order contributions from the coil, and are equivalent to the vector field generated by a linear current. The second terms are influences from the curvature of the coil, $1/a$, and the uniform magnetic field, B_x . If any one of these second terms is 0, the orbits form closed curves, whereas if both have nonzero finite values, the orbits form an unstable (stable) spiral around the singular point $(\tilde{z}, \tilde{x}) = (0, 0)$ for $B_x > 0$ ($B_x < 0$) [see the inset of Fig. 1(e)].

Although the point $(\tilde{z}, \tilde{x}) = (0, 0)$ of Eqs. (4) and (5) is a singular point, it can be regularized by a standard procedure [26]. In fact, by changing the time scales as $dt/ds = r^2/C$, we obtain the regularized equations

$$\frac{d\tilde{z}}{ds} = -\tilde{x} - \frac{1}{2a} \tilde{r}^2 \ln \tilde{r}^2, \quad (6)$$

$$\frac{d\tilde{x}}{ds} = \tilde{z} + \frac{B_x}{C} \tilde{r}^2, \quad (7)$$

where $\tilde{r} > 0$ is defined by $\tilde{r}^2 = \tilde{z}^2 + \tilde{x}^2$. The stability of the fixed point $(\tilde{z}, \tilde{x}) = (0, 0)$ of these equations cannot be analyzed by linear analysis, because the linearized equations are equivalent to the equations of a harmonic oscillator. Therefore we perform a weak nonlinear stability analysis using a Lyapunov function [27,28]. Let us define a scalar function $L(\tilde{z}, \tilde{x})$ as follows:

$$L = \tilde{r}^2 \left[\frac{1}{2} - \frac{B_x}{C} \tilde{z} - \frac{B_x^2}{C^2} \tilde{x}^2 \right] + \frac{\alpha B_x}{aC} (\tilde{x}^2 - \tilde{z}^2) \tilde{x} \tilde{z} \\ + \tilde{r}^2 \ln \tilde{r}^2 \left[\frac{\tilde{x}}{2a} + \frac{\tilde{x}^2}{4a^2} - \frac{B_x}{aC} \tilde{x} \tilde{z} \right] + \frac{\tilde{x}^2 \tilde{r}^2}{4a^2} (\ln \tilde{r}^2)^2,$$

where $\alpha = (2 - \sqrt{2})/8$. For $\tilde{z}, \tilde{x} \ll 1$, the function $L(\tilde{z}, \tilde{x})$ is positive, $L(\tilde{z}, \tilde{x}) \approx \tilde{r}^2/2 > 0$, except at the origin, where $L(\tilde{z}, \tilde{x}) = 0$. Moreover, the derivative with respect to s can be approximated as $dL/ds \approx \alpha B_x (\tilde{z}^2 + \beta \tilde{x}^2)^2/a$, where β is a constant defined by $\beta = 1 + 2\sqrt{2}$. Thus, for $B_x > 0$, we have $dL/ds > 0$ and hence the fixed point is unstable; for $B_x < 0$, we have $dL/ds < 0$ and hence the fixed point is stable. These results are consistent with the numerical simulations.

Here let us consider the following question: is the scattering process of this system chaotic? For the Hamiltonian systems with chaotic phase space, fractal structures usually appear in escape times $T(\mathbf{r}_i)$ of the the scattering orbits when $T(\mathbf{r}_i)$ is plotted as a function of initial coordinates $\mathbf{r}_i = (x_i, y_i, z_i)$ [7,29,30]. This is caused by fractal repellers (unstable periodic orbits) or fractal phase space structures such as the fractal island torus. In the present system with two actions, however, neither fractal repellers nor island torus exist, and in fact no fractal behavior is observed in the escape times $T(\mathbf{r}_i)$. Nevertheless, there are still some chaotic features in the scattering process.

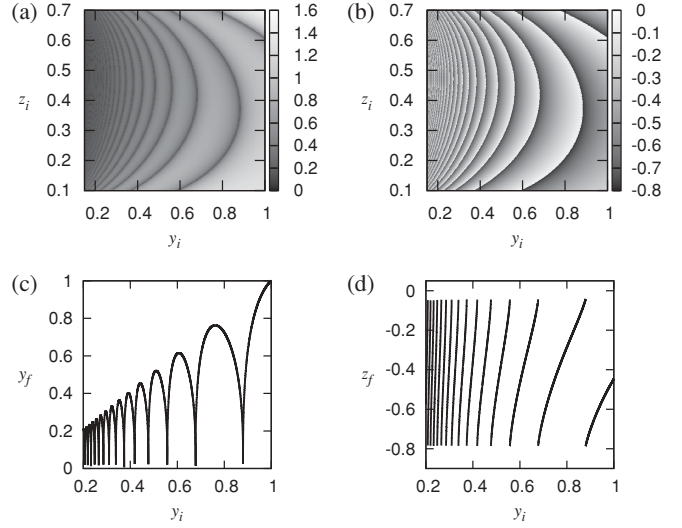


FIG. 2. For the single coil system with a uniform magnetic field, the two-dimensional scattering map $(y_f, z_f) = S(y_i, z_i)$ is displayed (see the text). The parameters are set as $I_C = 0.1, I_L = 0.0$, and $B_x = 0.005$ (two-action case). The values of the final coordinates y_f (a) and z_f (b) are shown in grayscale; the horizontal and vertical axes are the initial coordinates y_i and z_i , respectively. In (c) and (d), the final coordinates y_f (c) and z_f (d) are shown as functions of y_i , while the value of z_i is fixed to 0.4.

In order to see these chaotic properties, let us define the initial coordinates as $\mathbf{r}_i = (x_i = -2, y_i, z_i)$, and let $\mathbf{r}_f = (x_f = 2, y_f, z_f)$ be the final coordinates of the MFL starting from \mathbf{r}_i . This defines a two-dimensional map $S: (y_f, z_f) = S(y_i, z_i)$. In Figs. 2(a) and 2(b) we plotted the values of y_f and z_f as functions of the initial coordinates (y_i, z_i) , respectively. Similarly, in Figs. 2(c) and 2(d), y_f and z_f are plotted as functions of y_i , while z_i is fixed to 0.4. From Figs. 2(a) and 2(c), we found that the final coordinate y_f changes almost continuously (not smoothly), but as shown in Figs. 2(b) and 2(d) z_f changes discontinuously at some points. This means that the final coordinates depend sensitively on the changes of initial coordinates, which is a familiar feature of chaos. Moreover the mapping from the initial to final coordinates $S(y_i, z_i)$ depicted in Figs. 2(c) and 2(d) shows repetitive structures, and each piece of this repetition is qualitatively similar to the well-known chaotic dynamical systems called logistic and Bernoulli maps [31,32].

III. PARALLEL COIL SYSTEM

For the single coil system, chaos appears through the Poincaré-Birkhoff scenario, but for systems with parallel current elements, other scenarios are also important [7,33,34]. Here we study the system shown in Fig. 3(a), which consists of two parallel coils with their centers on the z axis and a straight wire along this axis. This type of current configuration is used, for example, in magneto-optical traps [5]. We assume that the intensities I_C and the directions of the currents carried by the two coils are the same, and that one of the coils is located on the xy plane and the other at $z = a$. Because this system, similar to the previous system, has rotational symmetry around the z axis, the equations for the MFLs are transformed into a

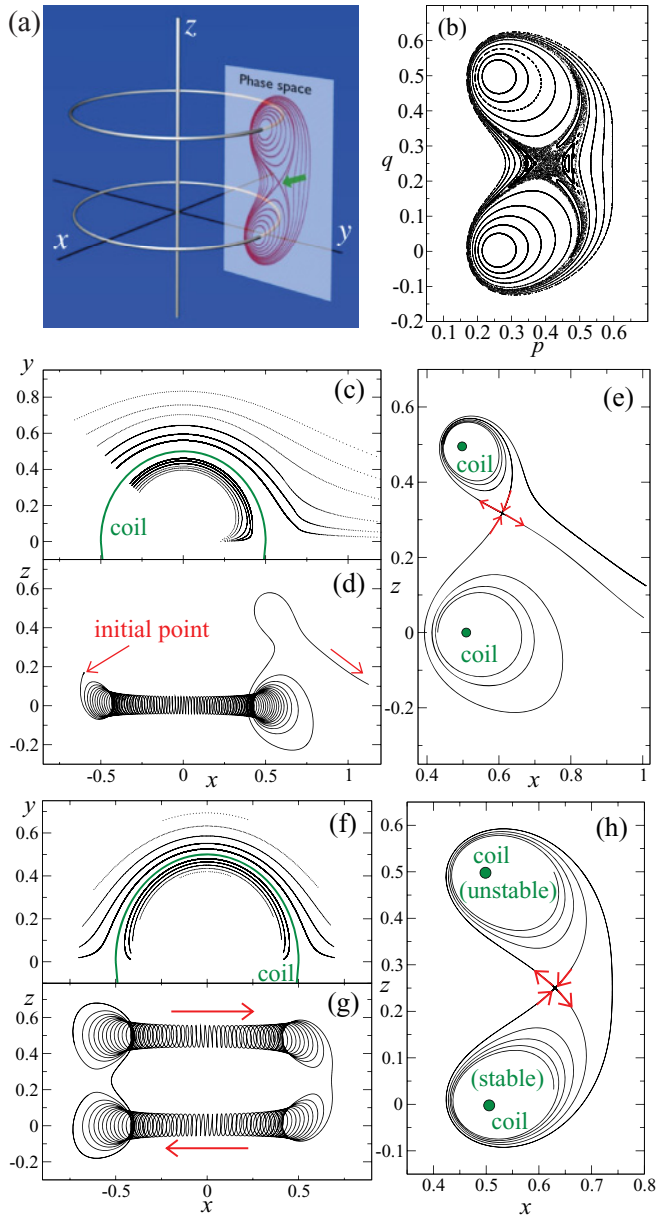


FIG. 3. (Color online) (a) The wire configuration of the parallel coil system. A hyperbolic fixed point is indicated by an arrow. (b) The Poincaré surface $\phi = \pi/2$ in the one-action case. The parameters are set as $I_C = I_L = 1.0$ and $B_x = 0.002$. (c)–(e) For two-action cases with uniform magnetic fields $\mathbf{B}_p = (B_x, 0, 0)$. The current intensities are set as $I_C = 0.1$ and $I_L = 0$. (c) A Poincaré section $z = 0$ for six orbits that start from the points $(-r_0/\sqrt{2}, r_0/\sqrt{2}, 0)$ ($0.38 \leq r_0 \leq 0.455$). The strength of the uniform magnetic field is set as $B_x = 0.0002$. (d) A projection of a typical orbit with positive y values onto the xz plane for $B_x = 0.02$. (e) The hyperbolic fixed point, and stable and unstable manifolds on the invariant subspace $\phi = 0$ for $B_x = 0.02$. The arrows indicate the directions of the stable and unstable manifolds. (f)–(h) For two-action cases with nonuniform magnetic fields $\mathbf{B}_p = ((z - a/2)B_x, 0, 0)$. (f) A Poincaré section $z = 0$ for six orbits that start from the points $(-r_0/\sqrt{2}, r_0/\sqrt{2}, 0)$ ($0.38 \leq r_0 \leq 0.455$). The strength of the uniform magnetic field is set as $B_x = 0.005$. (g) A projection of a typical orbit with positive y values onto the xz plane for $B_x = 0.02$. (h) The hyperbolic fixed point, and stable and unstable manifolds on the invariant subspace $\phi = 0$ for $B_x = 0.05$.

one-degree-of-freedom Hamiltonian form, Eqs. (3). The phase space of this system on the surface $\phi = \pi/2$ is shown in Fig. 3(a). Important aspects of this system are that a hyperbolic fixed point is present, as indicated by an arrow in Fig. 3(a), and that homoclinic orbits emanate from it. The emergence of such a hyperbolic fixed point is due to the presence of parallel electric currents.

As before, we use a uniform magnetic field $\mathbf{B}_p = (B_x, 0, 0)$ as a perturbation. First, in the case where there is a linear current ($I_L \neq 0$), corresponding to the one-action case, the Poincaré surface ($\phi = \pi/2$) is shown in Fig. 3(b). It is clear that chaos appears in a vicinity of the hyperbolic fixed point, and the cause of chaos can be considered to be homoclinic intersections of the stable and unstable manifolds. In regions far from the hyperbolic fixed points, however, the tori are persistent under the perturbation, consistent with the prediction of the KAM theorem. See Refs. [7,33,34] for more detail.

In the case where there is no linear current ($I_L = 0$), MFLs of the parallel coil system behave in a similar manner to those of the single coil. Namely, for arbitrarily weak perturbations, each periodic orbit of the unperturbed system is destroyed; the perturbed orbits circle around one of the coils transiently and then drift in the x direction ($B_x > 0$), as shown in Figs. 3(c) and 3(d). From numerical calculations, no chaotic transition between the upper and lower coils is found. When these orbits come close to the invariant subspace $\phi = 0$, they spiral out from one of the coils as is the case for the single coil system. In this case, however, the structure of the invariant subspace is more complex than in the previous case as shown in Fig. 3(e); in this figure, each stable manifold of the hyperbolic fixed point spirals out from one of the coils, and two unstable manifolds emanate from the hyperbolic fixed point. The bifurcations of the fixed points, $(z, x) = (0, a)$ and (a, a) , are the same type as in the single coil system. In fact, they are characterized by the same Lyapunov function $L(\tilde{z}, \tilde{x})$. It is important to note that similar instability results from other types of perturbations such as inclination or symmetry-breaking parallel translation of one of the coils.

However, such vanishing of all periodic orbits is not always the case. For example, if we apply a nonuniform magnetic field $\mathbf{B}_p = ((z - a/2)B_x, 0, 0)$ as a perturbation, then periodic orbits exist. A typical periodic orbit of this type is shown in Fig. 3(g); the orbit twining one of the coils transits to the other near the invariant subspaces $\phi = 0, \pi$. The remarkable point is that these are closed periodic orbits; in other words, none of the periodic orbits forms an invariant two-dimensional surface such as a torus. This is because, if an orbit forms an invariant surface, such as a tube around a coil, this surface will intersect with the coils at the transitions near the invariant subspaces.

IV. CONCLUSION

In this paper, two models for MFLs were investigated. The first one was a system consisting of a single coil and a straight wire with the linear current I_L . In the one-action case ($I_L \neq 0$), this model exhibits chaotic behavior similar to that in Hamiltonian systems. In contrast, in the two-action case ($I_L = 0$), all the periodic orbits of the unperturbed system vanish under a perturbation of a uniform magnetic field.

This phenomena was analyzed using a Lyapunov function, and it was found that a bifurcation associated with nonlinear effects occurs. The second model was a system consisting of two parallel coils and a straight wire, again with I_L . For the one-action case ($I_L \neq 0$), this system has a hyperbolic fixed point, which causes chaotic behavior through homoclinic intersection. It is also found that the scattering process shows sensitive dependence on small changes of the initial coordinates. In particular, the map from initial to final coordinates has structures similar to chaotic maps. In the two-action case ($I_L = 0$), it was found that the periodic orbits vanish under arbitrarily small perturbations of uniform magnetic fields due to a bifurcation similar to that in the single coil system. However, if the two fixed points on the invariant subspace have different stability types, which is the case for some perturbations of nonuniform magnetic fields, it was found that closed periodic orbits exist.

The bifurcations which emerged in two-action cases are typical in dissipative systems, but not usually observed in Hamiltonian systems.¹ It is interesting that characteristics

¹The bifurcations observed in the invariant subspaces of the two-action cases are roughly characterized by the following changes of the eigenvalues of the fixed point: $(\pm i\beta) \rightarrow (\alpha \pm i\beta)$, where α and

of both Hamiltonian and dissipative systems appear in these models. From a linear stability analysis of three-dimensional volume-preserving flows and maps with two action variables, the existence of bifurcation similar to that described in this paper has been reported [20]. In the models used in the present work, however, the bifurcation occurs through nonlinear effects.

ACKNOWLEDGMENTS

We thank anonymous referees for valuable comments and helpful suggestions. K.N. is grateful for financial support from a project of the Uzbek Academy of Sciences (Grant No. FA-F2-084).

β are real numbers. Obviously, this type of bifurcation does not occur in one-degree-of-freedom Hamiltonian systems because of the conservation of the phase volume. However, in Hamiltonian systems with two or more degrees of freedom, the following bifurcation can happen: $(\pm i\beta, \pm i\beta) \rightarrow (-\alpha \pm i\beta, \alpha \pm i\beta)$. This bifurcation is similar to the one observed in the models of this paper, but this is not generic in Hamiltonian systems in the sense that there should be degeneracies of the eigenvalues $(\pm i\beta, \pm i\beta)$ in the unperturbed system.

-
- [1] P. J. Morrison, *Phys. Plasmas* **7**, 2279 (2000).
 [2] J. Aguirre and D. Peralta-Salas, *Europhys. Lett.* **80**, 60007 (2007).
 [3] M. Hosoda, T. Miyaguchi, K. Imagawa, and K. Nakamura, *Phys. Rev. E* **80**, 067202 (2009).
 [4] A. Thess, E. V. Votyakov, and Y. Kolesnikov, *Phys. Rev. Lett.* **96**, 164501 (2006).
 [5] T. Bergeman, G. Erez, and H. J. Metcalf, *Phys. Rev. A* **35**, 1535 (1987).
 [6] A. H. Boozer, *Rev. Mod. Phys.* **76**, 1071 (2005).
 [7] S. S. Abdullaev, *Construction of Mappings for Hamiltonian Systems and Their Applications* (Springer-Verlag, Berlin, 2006).
 [8] G. M. Zaslavsky, *Hamiltonian Chaos & Fractional Dynamics* (Oxford University Press, New York, 2005), Chaps. 2 and 23.
 [9] M. Feingold, L. P. Kadanoff, and O. Piro, *J. Stat. Phys.* **50**, 529 (1988).
 [10] J. H. E. Cartwright, M. Feingold, and O. Piro, *Phys. Rev. Lett.* **75**, 3669 (1995).
 [11] J. M. Ottino, C. W. Leong, H. Rising, and P. D. Swanson, *Nature (London)* **333**, 419 (1988).
 [12] K. Bajer and H. K. Moffatt, *J. Fluid Mech.* **212**, 337 (1990).
 [13] T. H. Solomon, E. R. Weeks, and H. L. Swinney, *Phys. Rev. Lett.* **71**, 3975 (1993).
 [14] G. O. Fountain, D. V. Khakhar, and J. M. Ottino, *Science* **281**, 683 (1998).
 [15] T. H. Solomon and I. Mezić, *Nature (London)* **425**, 376 (2003).
 [16] V. I. Arnold, C. R. Hebd. Seances Acad. Sci. **261**, 17 (1965).
 [17] I. Mezić and S. Wiggins, *J. Nonlinear Sci.* **4**, 157 (1994).
 [18] J. Aguirre, J. Giné, and D. Peralta-Salas, *Nonlinearity* **21**, 51 (2008).
 [19] A. J. Lichtenberg and M. A. Lieberman, *Regular and Chaotic Dynamics*, 2nd ed. (Springer-Verlag, New York, 1992).
 [20] I. Mezić, *Physica D* **154**, 51 (2001).
 [21] D. L. Vainchtein, J. Widloski, and R. O. Grigoriev, *Phys. Rev. Lett.* **99**, 094501 (2007).
 [22] D. L. Vainchtein, J. Widloski, and R. O. Grigoriev, *Phys. Rev. E* **78**, 026302 (2008).
 [23] J. D. Jackson, *Classical Electrodynamics*, 3rd ed. (Wiley, New York, 1998), Chap. 5.
 [24] L. D. Landau, L. P. Pitevskii, and E. M. Lifshitz, *Electrodynamics of Continuous Media*, 2nd ed. (Elsevier, Oxford, 1984), Chap. 30.
 [25] F. G. Gascón and D. Peralta-Salas, *Physica D* **206**, 109 (2005).
 [26] E. L. Stiefel and G. Scheifel, *Linear and Regular Celestial Mechanics* (Springer-Verlag, Berlin, 1971).
 [27] J. Guckenheimer and P. Holmes, *Nonlinear Oscillations, Dynamical Systems, and Bifurcations of Vector Fields* (Springer-Verlag, New York, 1997).
 [28] S. Wiggins, *Introduction to Applied Nonlinear Dynamical Systems and Chaos*, 3rd ed. (Springer-Verlag, 1997).
 [29] P. Gaspard, *Chaos, Scattering and Statistical Mechanics* (Cambridge University Press, Cambridge, 1998).
 [30] M. Ding, C. Grebogi, E. Ott, and J. A. Yorke, *Phys. Rev. A* **42**, 7025 (1990).
 [31] J. R. Dorfman, *An Introduction to Chaos in Non-Equilibrium Statistical Mechanics* (Cambridge University Press, Cambridge, 1999).
 [32] T. Miyaguchi, *Prog. Theor. Phys.* **115**, 31 (2006).
 [33] Y. Tomita, S. Seki, and H. Momota, *J. Phys. Soc. Jpn.* **42**, 687 (1977).
 [34] Y. Tomita, Y. Nomura, H. Momota, and R. Itatani, *J. Phys. Soc. Jpn.* **44**, 637 (1978).